Doubly excited resonance states of helium in exponential cosine-screened Coulomb potentials

Arijit Ghoshal* and Y. K. Ho
Institute of Atomic and Molecular Sciences, Academia Sinica, P.O. Box 23-166, Taipei, Taiwan 106, Republic of China
(Received 5 March 2009; published 26 June 2009)

We have made an investigation on the $2s^2\ ^1S^e$ resonances in helium (He) in exponential cosine-screened Coulomb potentials (ECSCP). Highly correlated wave functions are used to take into account of the correlation effect of the charged particles. Resonance energies and widths for the doubly excited He in ECSCP are determined using the stabilization method by calculating the density of the resonance states. Results for resonance energies and widths are reported for the screening parameter in the range 0.0–0.275

DOI: 10.1103/PhysRevA.79.062514 PACS number(s): 32.30.−r, 34.80.Dp, 52.20.−j

I. INTRODUCTION

The study of atomic phenomena under the influence of an environment is of utmost importance. Because an isolated atom or ion may behave very differently from those under the influence of an environment, the energy spectrum and other properties may change considerably. The changes in the properties depend on the interaction between the atom and its surroundings (Ref. [1] and further references therein). Such interaction is a measure of the influence of the environment on the atom or ion, and to some extent can be represented by model potentials. For example, the electronic structure of ions embedded in weakly coupled plasmas can be modeled by screened Coulomb potentials (SCP) with screening parameter, λ [2],

$$V(r) = (-1/r)e^{-\lambda r} \quad \text{(in a.u.)}, \tag{1}$$

rather than the pure Coulomb one (PCP). The screening parameter λ shortens the range of the potential in comparison to the pure Coulomb case. The effects of screened Coulomb interaction between charged particles in plasmas on atomic structure and collision properties have been the subject of extensive studies in the last four decades (Refs. [3–9] and further references therein). These studies have been motivated mainly by the research in laser-produced plasmas, EUV, and x-ray laser development, and inertial confinement fusion and astrophysics. Again the effective potential for a test charge in dense quantum plasma can be modeled by modified Debye-Hückel potential or exponential cosine-screened Coulomb potential (ECSCP) [10] with screening parameter λ,

$$V(r) = (-1/r)e^{-\lambda r}\cos(\lambda r) \quad \text{(in a.u.)}, \tag{2}$$

rather than SCP. Usually, quantum plasmas are characterized by a low-temperature and a high-number density. In such quantum plasmas, λ is related to the quantum wave number of the electron, which, in turn, is related to the electron plasma frequency. For weakly coupled plasmas, $\cos(\lambda r)$ term in Eq. (2) is absent, and so it becomes SCP as in Eq. (1). Due to the presence of the cos term in ECSCP, it exhibits stronger screening effect than SCP. An exponential cosine-screened Coulomb potential not only represents the effective interaction between the charged particles in a dense quantum plasma, but also is known to represent the potential between an ionized impurity and an electron in metal [12–15], and the ionized impurity-electron potential in a semiconductor [16,17]. Furthermore, ECSCP are also found to exist in various nanoscale objects, such as nanowires, quantum dot, semiconductor devices, and laser-produced dense plasmas [10,11]. Nowadays these potentials find increasing applications in various physics research areas, such as solid-state physics [12–19], nuclear physics [20,21], and plasma physics [10,11,22–24].

In this paper our objective is to investigate the $2s^2\ ^1S^e$ autoionization resonance states of He in ECSCP. There is, of course, a continuous interest in investigate atomic resonance phenomena of two-electron systems [25–32]. Moreover, investigation on two-electron system in ECSCP plays an important role because correlation effects between the charged particles can be studied. Recently we have determined the ground-state energies and wave functions of He in ECSCP [33]. In SCP, $2s^2\ ^1S^e$ autoionization resonance states of He have been investigated by Kar and Ho [30], but in ECSCP, to the best of our knowledge, no such investigation on resonances in a two-electron system has been reported so far in the literature.

The plan of this paper is as follows: describing the underlying theory and calculations of our investigation in Sec. II; we present and discuss our computed results in Sec. III. Finally, in Sec. IV we give our concluding remarks.

The atomic units (a.u.) are used throughout the present work, and all calculations are performed in quadruple precision (32 significant figures) on IBM-AMD workstations in UNIX environment.

II. THEORY AND CALCULATIONS

The nonrelativistic Hamiltonian of He in ECSCP characterized by the screening parameter λ is given by

$$H = -\frac{1}{2}\nabla_1^2 - \frac{1}{2}\nabla_2^2 - 2\left[\frac{e^{-\lambda r_1}}{r_1}\cos(\lambda r_1) + \frac{e^{-\lambda r_2}}{r_2}\cos(\lambda r_2)\right] + \frac{e^{-\lambda r_{12}}}{r_{12}}\cos(\lambda r_{12}), \tag{3}$$

where $\mathbf{r}_1$ and $\mathbf{r}_2$ are the coordinates of the two electrons

*Permanent address: Department of Mathematics, Burdwan University, Golapbag, Burdwan 713 104, West Bengal, INDIA.

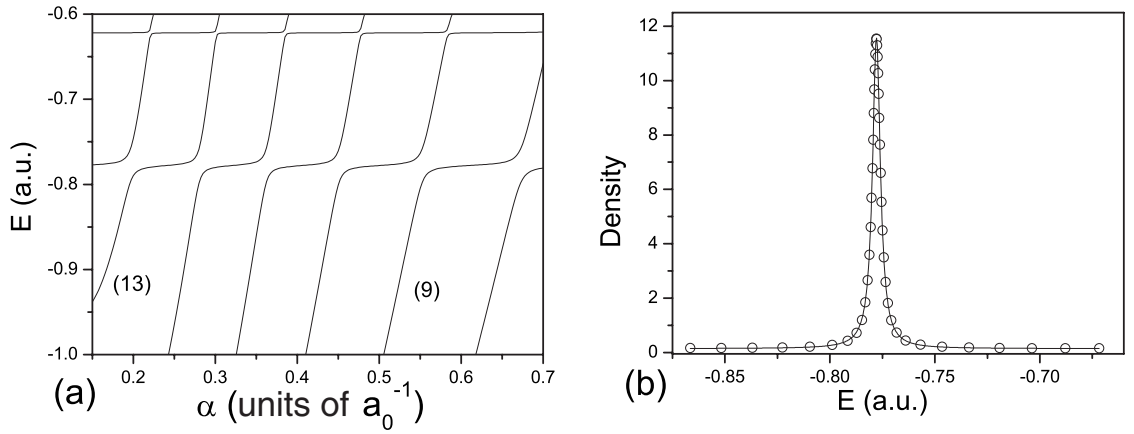

FIG. 1. (a) Stabilization plots of the $2s^2\ ^1S^e$ states of He in ECSCP for $\lambda=0.0$ and $\omega \leq 14(N=372)$. The number in the parenthesis next to the solid line indicates the order of appearance of the eigenvalues. (b) Calculated density (circles) and the fitted Lorenztian (solid line) for 12th eigenvalue corresponding to the $2s^2\ ^1S^e$ state of He in ECSCP for $\lambda=0.0$.

relative to the nucleus (assumed to be at rest), and $\mathbf{r}_{12}$ is their relative distance. The screening parameter λ determines the effect of screening. With the increase of λ the screening becomes stronger.

In order to determine $^1S^e$ states of He atom in ECSCP, we have employed the wave-function

$$\Psi(\mathbf{r}_1,\mathbf{r}_2) = \sum_{i=1}^{N} C_i \psi_i = \sum_{i=1}^{N} C_i (1+P_{12}) e^{-A(r_1+r_2)\alpha} r_1^{l_i} r_2^{m_i} r_{12}^{n_i}, \tag{4}$$

$$l_i, m_i, n_i = 0,1,2,\cdots,$$

$$l_i \geq m_i,$$

where A is a nonlinear variational parameter, $C_i (i=1,2,3,\cdots,N)$ are linear-expansion coefficients, α is a scaling constant to be discussed later, and P_{12} is an exchange operator such that $P_{12} f(\mathbf{r}_1,\mathbf{r}_2)=f(\mathbf{r}_2,\mathbf{r}_1)$ for an arbitrary function f. Such a correlated wave function of general type has recently been used by us [33] to determine the ground-state energies and wave functions of He in ECSCP. This wave function has been expanded by generating the powers of r_1, r_2, and r_{12} in such a way that the terms corresponding to $l_i+m_i+n_i=\omega=0(N=1)$ come first, then $\omega \leq 1(N=3)$, $\omega \leq 2(N=7)$, and so on. To determine the ground-state energies of He in ECSCP we have first set $\alpha=1$. The nonlinear variational parameter A has then been optimized using Monte Carlo optimization technique within the framework of Ritz's variational principle [34].

In order to determine the resonance energies and widths, we have used stabilization method similar to Kar and Ho [27]. This method is a slight generalization of the stabilization method proposed by Mandelshtam *et al.* [32]. First, after diagonalization of the Hamiltonian (3) using the wave function (4) with different values of α (other than $\alpha=1$), we have obtained the energy levels $E(\alpha)$ for a particular value of λ. We then construct stabilization diagrams [as shown in Figs. 1(a), 2(a), and 3(a)] by plotting $E(\alpha)$ versus α. If there is a resonance at energy E, the stabilized or slowly decreasing energy levels will appear in the stabilization plateau. The details of successful applications of this simple and efficient method are available in the works of Ho and Kar (Ref. [27]

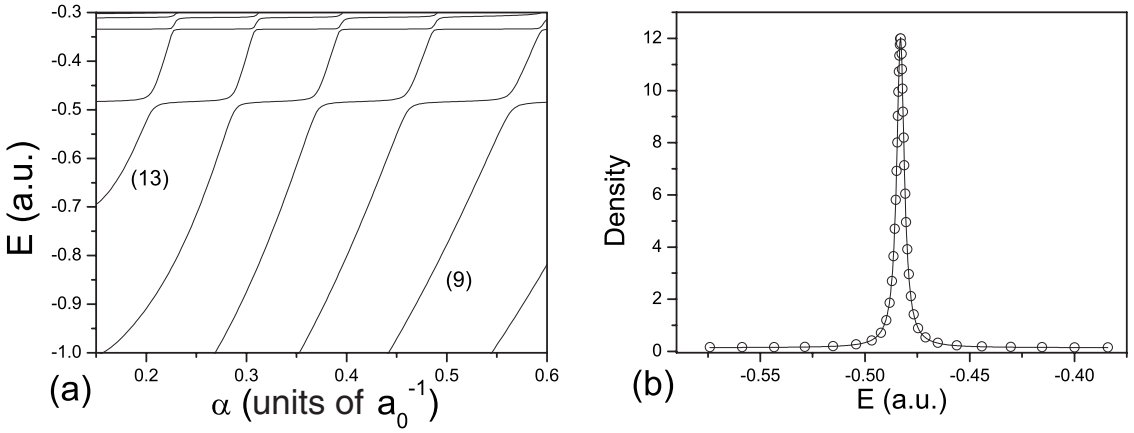

FIG. 2. (a) Stabilization plots of the $2s^2\ ^1S^e$ states of He in ECSCP for $\lambda=0.1$ and $\omega \leq 14(N=372)$. The number in the parenthesis next to the solid line indicates the order of appearance of the eigenvalues. (b) Calculated density (circles) and the fitted Lorenztian (solid line) for the 12th eigenvalue corresponding to the $2s^2\ ^1S^e$ state of He in ECSCP for $\lambda=0.1$.

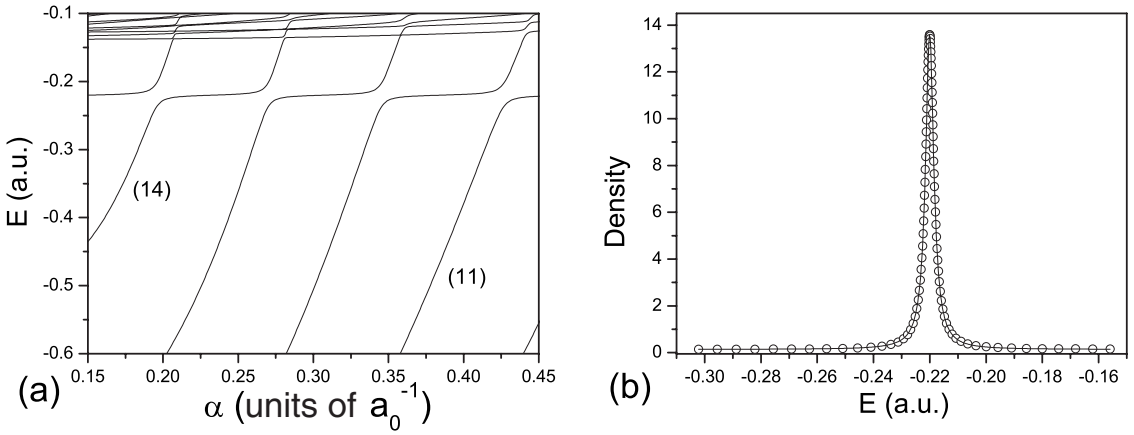

FIG. 3. (a) Stabilization plots of the $2s^2\ ^1S^e$ states of He in ECSCP for $\lambda=0.2$, and $\omega \leq 15(N=444)$. The number in the parenthesis next to the solid line indicates the order of appearance of the eigenvalues. (b) Calculated density (circles) and the fitted Lorenztian (solid line) for the 13th eigenvalue corresponding to the $2s^2\ ^1S^e$ state of He in ECSCP for $\lambda=0.2$.

and further references therein). The scaling parameter α in the wave function (4) can be considered as the reciprocal range of a "soft" wall [27,28]. By changing the range of the "soft wall," we obtain different energy levels $E(\alpha)$ which lead to stabilization plots. It is worthy to mention here that, in the original work of Mandelshtam *et al.* [32], a particle-in-a-box approach was used to calculate resonances for a short-range model potential. A fixed wave function was used, and the range of the potential was "cut-off" after the box size had reached a sufficiently large value. In our present work for a real atomic system, placing the atom inside a hard wall leads to computational difficulty. So we take an alternate approach by keeping the potential in the Hamiltonian fixed, but the wave function is changed by varying the nonlinear parameter α in the wave function. If the employed wave function is capable of representing the "physics" of the system, and the basis set of the wave function is sufficiently large to cover the effective range that the potential spans, a stabilization plateau in the stabilization plot would reveal the existence of a resonance.

Next, to extract the resonance-energy E_r and the resonance-width Γ, we have calculated the density of resonance states for a single energy level with the help of the following formula:

$$\rho_n(E) = \left[\frac{E_n(\alpha_{i+1}) - E_n(\alpha_{i-1})}{\alpha_{i+1} - \alpha_{i-1}}\right]^{-1}_{E_n(\alpha_i)=E}, \tag{5}$$

where the index i is the ith value for α and the index n is for the nth resonance. After calculating the density of resonance-states $\rho_n(E)$ with the above formula, we fit it to the following Lorentzian form:

TABLE I. Resonance energies (a.u.) and width (a.u.) along with χ^2 and r^2 arising out of the Lorentz fitting of different eigenvalues corresponding to $\lambda=0.0$ and $\lambda=0.1$. 372 terms are used to draw the stabilization plot in the range $0.2 \leq \alpha \leq 0.7$ and $0.2 \leq \alpha \leq 0.6$, respectively, which are covered by mesh points with the size 0.0025 (see Figs. 1 and 2). $\delta|E| = [|E_r^{\mathrm{CCR}} - E_r^{\mathrm{st}}|^2 + (1/4)|\Gamma^{\mathrm{CCR}} - \Gamma^{\mathrm{st}}|^2]^{1/2}$, where CCR and st denote that the corresponding quantities are obtained from the method of complex coordinate rotation (Ref. [26]) and present stabilization method.

Eigenvalue number	$-E_r$	Γ	χ^2	r^2	$\delta\|E\|$
		$\lambda=0.0$			
9	0.77777	0.004527	0.00494	0.99988	0.00010021
10	0.77779	0.004517	0.00267	0.99991	0.00008082
11	0.77781	0.004510	0.00124	0.99995	0.00006185
12	0.77784	0.004503	0.00038	0.99998	0.00003525
13	0.77794	0.004578	0.00341	0.99983	0.00007253
		$\lambda=0.1$			
10	0.48301	0.004393	0.00299	0.99991	
11	0.48303	0.004386	0.00140	0.99994	
12	0.48306	0.004378	0.00052	0.99998	
13	0.48312	0.004426	0.00135	0.99993	

$$\rho_n(E) = y_0 + \frac{\delta}{\pi} \frac{\frac{\Gamma}{2}}{(E - E_r)^2 + \left(\frac{\Gamma}{2}\right)^2}, \tag{6}$$

where y_0 is the baseline offset, δ is the total area under the curve from the base line, E_r is the center of the peak, and Γ denotes the full width of the peak of the curve at half height. This Lorentzian fitting gives us resonance-energy E_r and resonance-width Γ. In the present work, instead of using the averaging formula given by Mandelshtam *et al.* [32], we use Eq. (5) to calculate the density of resonance states from the stabilization plots, with one plateau at a time. The calculated density of resonance states from the individual plateau is then fitted to Eq. (6), and the one that gives the best fit (with the least χ square) to the Lorentzian form is considered as the desired result for that particular resonance.

III. RESULTS AND DISCUSSION

In order to construct the stabilization plot, we use an expansion length of $\omega \leq 14(N=372)$ of the wave function (4). The stabilization diagram, in Fig. 1(a), corresponding to $\lambda = 0.0$ in the range of $\alpha = 0.15-0.7$ shows the stabilization character near $E \approx -0.77$. This range of α is covered by 221 points in the mesh size of 0.0025. We have calculated the density of resonance states for the individual energy levels in the range 0.15–0.7, with one energy level at a time. The calculated density of resonance states from the single-energy eigenvalue are then fitted to Eq. (6), and the one that gives the best fit (with the least χ^2) to the Lorentzian form is considered as the desired result for that particular resonance. It is to be noted that we are using a finite basis set to represent the wave function, so when the density of a stabilized energy level is fitted to Eq. (6), the fitting may not give the best result for all the stabilized energy levels. In Table I we present the results of fitting of different energy levels obtained by using 372 terms in the wave function corresponding to $\lambda = 0.0$ and $\lambda = 0.1$ in the range of $\alpha = 0.2-0.7$ and $\alpha = 0.2-0.6$, respectively [see Figs. 1(a) and 2(a)]. This table also exhibits the absolute difference of the resonance parameters, $\delta|E| = [|E_r^{\mathrm{CCR}} - E_r^{\mathrm{st}}|^2 + (1/4)|\Gamma^{\mathrm{CCR}} - \Gamma^{\mathrm{st}}|^2]^{1/2}$, where CCR and st denote that the corresponding quantities are obtained from the method of complex coordinate rotation [26] and the present stabilization method, corresponding to the different fittings for $\lambda = 0.0$. From this table we see that 12th eigenvalue gives the best fitting (least χ^2, $r^2 \approx 1$, and δE is the smallest for $\lambda = 0.0$) for both $\lambda = 0.0$ and $\lambda = 0.1$. Now Fig. 1(b) shows the fitting of the density of resonance states for the 12th eigenvalue of the stabilization plot [Fig. 1(a)]. From the fit, we obtain the resonance-energy $E_r = -0.77784$ and the corresponding width as $\Gamma = 0.004503$. The circles are the results of the actual calculations of the density of resonance states using formula (5), and the solid line is the fitted Lorentzian form of the corresponding Eq. (6). These results, for case of $\lambda = 0.0$, are also in nice agreement with those reported by Kar and Ho [30] using stabilization method. Furthermore, this resonance energy converted to electronvolt and measured from the ground state of the helium atom is 57.8 eV and the width when converted to electronvolt is 0.122 eV. These values compare quite well with the measured results, $E_r = 57.82 \pm 0.04$ eV and $\Gamma = 0.138 \pm 0.015$ eV, in an electron-impact experiment [31].

TABLE II. Convergence of the resonance energy (E_r) (a.u.) and width (Γ) (a.u.) with $\omega \leq 12(N=252)$, $\omega \leq 14(N=372)$, and $\omega \leq 15(N=444)$ corresponding to the screening parameter $\lambda = 0.2$. The fittings correspond to 11th, 13th, and 13th eigenvalue, where mesh points with 0.001 spacing is used.

	$\omega \leq 12$	$\omega \leq 14$	$\omega \leq 15$
$-E_r$	0.220059	0.220048	0.220048
Γ	0.003581	0.003587	0.003559

In order to check the convergency of our calculation we have constructed the stabilization plot for three different expansion lengths, namely, $\omega \leq 12(N=252)$, $\omega \leq 14(N=372)$, and $\omega \leq 15(N=444)$ of the wave function (4) in the range of $\alpha = 0.15-0.45$ for $\lambda = 0.2$. This range, $0.15 \leq \alpha \leq 0.45$, has been covered by 301 points in the mesh size of 0.001. In Table II we present the results of resonance parameters for these three expansions of the wave function (4). The numbers in this table establish the convergency of the resonance parameters with the increase in terms in the wave function. In Figs. 2(a) and 3(a) the stabilization plots for $\lambda = 0.1$ and $\lambda = 0.2$ are shown. The corresponding Lorenztian fittings are shown in Figs. 2(b) and 3(b), respectively. These plots have been made in the range of $0.15 \leq \alpha \leq 0.6$ and $0.15 \leq \alpha \leq 0.45$ with mesh sizes 0.0025 and 0.001, respectively. It is worthy to mention here that, when density of the resonance states $\rho_n(E)$ is fitted to the Lorentzian form, it is observed that the value of χ^2 for each fitting is much less than 0.1. The overall uncertainty in our present investigation is about 4×10^{-5} a.u. each for the resonance energy and width.

In Table III, we present the resonance energies and the widths for some values of the screening parameter λ ranging from zero (corresponding to no screening) to 0.275 (corresponding to strong screening) along with the energies of $\mathrm{He}^+(2s)$. All these results have been obtained using 372 terms in the wave function. The values of the $\mathrm{He}^+(2s)$ energies have been calculated by using a wave function of the form

$$\Psi(\mathbf{r}) = \sum_i C_i \psi_i = \sum_i C_i e^{-A_i r} r^{l_i}, \quad l_i = 0, 1, 2, \cdots,$$

where A_i is a nonlinear variational parameter, and $\mathbf{r}$ denotes the coordinates of the electron relative to the nucleus, within

TABLE III. The resonance energies (E_r) (a.u.) and widths (Γ) (a.u.) along with the energies of $\mathrm{He}^+(2s)$ in ECSCP for various values of the screening parameter λ.

λ	$-E_{\mathrm{He}^+(2s)}$	$-E_r$	Γ
0.0	0.5	0.77784	0.004503
0.05	0.400793962	0.62848	0.004487
0.1	0.305798385	0.48306	0.004378
0.15	0.218026079	0.34554	0.004085
0.2	0.139765248	0.22004	0.003559
0.25	0.073148176	0.11142	0.002642
0.275	0.045030496	0.06560	0.002008

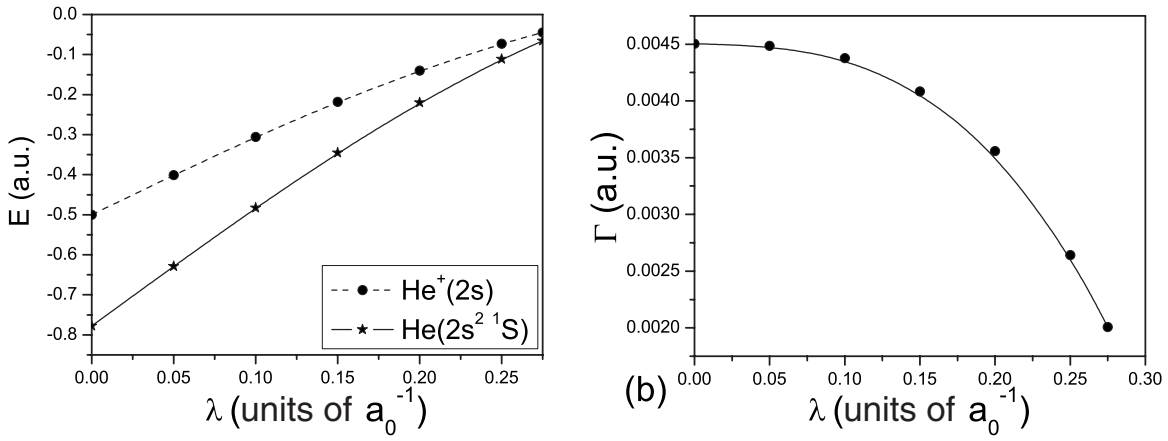

FIG. 4. (a) The $2s^2\ ^1S^e$ resonance energy E_r for different values of the screening parameter λ. Dashed line denotes the $He^+(2s)$ threshold energy. (b) Resonance width, Γ, corresponding to the resonance energy in (a) for different values of the screening parameter λ.

the frame work of Ritz's variational principle [34].

In Fig. 4(a) we have plotted the present resonance energies associated with the $N=2$ He^+ threshold along with the $He^+(2s)$ threshold energies for different values of λ. The corresponding widths are plotted in Fig. 4(b). From Fig. 4(a) and also from Table III, it is seen that the resonance energy gradually increases with increasing value of λ and ultimately becomes very close to $He^+(2s)$ energy at $\lambda=0.275$. It should be mentioned here that we have not found any Feshbach-type resonances lying below the $He^+(2s)$ threshold beyond $\lambda=0.3$. For $0.275<\lambda\leq 0.3$, the resonance, if existing, would be located very near the $He^+(2s)$ threshold as is evident from Fig. 4(a). However, such calculations would need more extensive basis sets, and are outside the scope of our present investigation.

Furthermore, from Table III and Fig. 4(b), it is seen that the resonance-width Γ decreases with increasing value of λ. Though a more quantitative explanation of this situation needs a separate investigation which is beyond the scope of the present paper, yet an attempt to explain such phenomenon can be made in the following way: For S-wave resonances lying below the $He^+(N=2)$ threshold, they can be classified into "+" and "−" states. Readers are referred to Refs. [35,36] and the references therein for detailed discussions. The + state corresponds to the radial motions of the two electrons in step with one another, and the − state corresponds to the radial motions of the two electrons out of step with one another. The $2s^2\ ^1S^e$ state in He is a + state, and the two electrons are located on the opposite sides of the nucleus. The movements of the two electrons are such that they are moving toward the nucleus "in phase." The autoionization of such a state is accomplished through momentum transfer, as one of the electrons is "knocked out" by the other via the nucleus. When the electron-ion screening is increased (increasing λ), the attractive force is reduced. But at the same time, increasing the electron-electron screening would result in the decrease in the repulsive force. Apparently, the screening has a larger effect on the electron-ion attraction than on the electron-electron repulsion. As a result, the movement of the electrons will be slowed down, and the lifetime of the autoionization process will be prolonged, leading to the narrowing of the resonance width, a consequence of the uncertainty principle. Alternatively, this can also be described by the mixing of configuration spaces belonging to a discrete spectrum (the so-called closed space $Q\Psi$ in the Feshbach projection formulism) with continuous spectrum (the so-called open-space $P\Psi$ in the Feshbach projection formulism), which gives rise to the phenomenon of autoionization [37] by ejecting an electron. The resonance width is given by $\Gamma=2\pi|V_E|^2$, where $|V_E|^2$ is an index of the strength of the configuration interaction [38]. $|V_E|^2$ is characterized by the product of two different factors, one is determined by the configuration interaction within the closed space of the doubly excited two-electron helium, whereas the other (the open space) is determined by the details of the field at large distance from the $He^+(1s)$ ground state, the state to which the doubly excited $2s^2\ ^1S^e$ resonance autoionized. Now as the screening increases, it seems that both these factors decrease and as a result the width decreases. Furthermore, from Fig. 4(a), it is observed that the resonance energy approaches toward a bound state of He^+ ion as λ increases. In other words, as the screening increases, it looks like pressure ionization may occur. At the limit, one has a bound state, and its width becomes zero [39]. The second S-wave resonance state, denoted by $2p^2\ ^1S^e$, is classified as a − state. The screening effect on such a state will have a different consequence, and it is outside the scope of our present investigation to study the − states. Again, here we should mention that the above discussion for the screening effect on the resonance widths is a conjecture, and we have not carried out detailed analysis for the resonance wave functions under the external screening environments. It seems such investigations are called for, and we hope that our findings would stimulate further studies of such intriguing phenomenon.

In Table IV we have compared our present results of ECSCP with those of Kar and Ho using SCP [30]. From this table we notice that the resonance energy (and the excited $2S$ state energy) at a particular value of λ is being shifted to a higher-resonance position in ECSCP than in SCP. This is quite expected due to the stronger screening effect of ECSCP than of SCP.

IV. CONCLUSIONS

We have carried out a calculation on the $2s^2\ ^1S^e$ autoionization resonances for helium atom interacting with exponen-

TABLE IV. The resonance energies (E_r) (a.u.) and widths (Γ) (a.u.) of He in ECSCP and SCP for various values of the screening parameter λ.

Potential	$\lambda \Rightarrow$	0.0	0.05	0.1	0.2	0.25
$-E_r$	ECSCP[a]	0.77784	0.62848	0.48306	0.22004	0.11142
	SCP[b]	0.77783	0.63683	0.51279	0.31105	0.23151
	PCP[c]	0.77787				
Γ	ECSCP[a]	0.004503	0.004487	0.004378	0.003559	0.002642
	SCP[b]	0.004549	0.004450	0.004159	0.003191	0.002591
	PCP[c]	0.00454				

[a]Present results.
[b]SCP results of Kar and Ho using 500 terms in the basis set (Ref. [30]).
[c]PCP results of Ho using the method of complex coordinate rotation with 308 terms in the wave function (Ref. [26]).

tial cosine-screened Coulomb potentials. Highly correlated Hylleraas-type wave functions have been employed to take into account the correlation effects. The resonance energies and widths for various values of the screening parameter ranging from 0 to 0.275 are reported in the present work. The stabilization method has been used to extract resonance energies and widths. This method is a computational powerful and practical method to determine resonance parameters (E_r, Γ). Our work on ECSCP will play a role in studies of atomic structures and collisions processes in quantum plasmas [10,24].

This work has been sponsored by the National Science Council of Taiwan, Republic of China. We would like to thank an anonymous referee for some helpful comments.

[1] W. Jaskolski, Phys. Rep. **271**, 1 (1996).
[2] L. Zhang and P. Winkler, Int. J. Quantum Chem. **S30**, 431 (1996).
[3] D. Salzman, *Atomic Physics in Hot Plasmas* (Oxford University Press, Oxford, 1998).
[4] M. S. Murillo and J. C. Weisheit, Phys. Rep. **302**, 1 (1998).
[5] L. Liu, J. G. Wang, and R. K. Janev, Phys. Rev. A **77**, 032709 (2008); **77**, 042712 (2008).
[6] M. S. Pindzola, S. D. Loch, J. Colgan, and C. J. Fontes, Phys. Rev. A **77**, 062707 (2008).
[7] Y. Y. Qi, J. G. Wang, and R. K. Janev, Phys. Rev. A **78**, 062511 (2008).
[8] S. Kar and Y. K. Ho, Phys. Rev. A **77**, 022713 (2008).
[9] S. Paul and Y. K. Ho, Phys. Rev. A **78**, 042711 (2008).
[10] P. K. Shukla and B. Eliasson, Phys. Lett. A **372**, 2897 (2008).
[11] M. Marklund and P. K. Shukla, Rev. Mod. Phys. **78**, 591 (2006).
[12] V. L. Bonch-Bruevich and V. B. Glasko, Sov. Phys. Dokl. **4**, 147 (1959).
[13] N. Takimoto, J. Phys. Soc. Jpn. **14**, 1142 (1959).
[14] E. C. McIrvine, J. Phys. Soc. Jpn. **15**, 928 (1960).
[15] G. L. Hall, Phys. Chem. Solids **23**, 1147 (1962).
[16] V. L. Bonch-Bruevich and Sh. M. Kogan, Sov. Phys. Solid State **1**, 1118 (1960).
[17] V. L. Bonch-Bruevich and S. V. Tyablikov, *The Green's Function Method in Statistical Mechanics* (North-Holland, Amsterdam, 1962), Chap. IV.
[18] E. P. Prokopev, Sov. Phys. Solid State **9**, 993 (1967).
[19] J. B. Krieger, Phys. Rev. **178**, 1337 (1969).
[20] H. Yukawa, Proc. Phys. Math. Soc. Jpn. **17**, 48 (1935).
[21] A. E. S. Green, Phys. Rev. **75**, 1926 (1949).
[22] H. Margenau and M. Lewis, Rev. Mod. Phys. **31**, 569 (1959).
[23] G. M. Harris, Phys. Rev. **125**, 1131 (1962).
[24] Sang-Chul Na and Young-Dae Jung, Phys. Lett. A **372**, 5605 (2008); Phys. Scr. **78**, 035502 (2008).
[25] C. D. Lin, Phys. Rev. Lett. **51**, 1348 (1983).
[26] Y. K. Ho, Phys. Rev. A **23**, 2137 (1981); **34**, 4402 (1986).
[27] S. Kar and Y. K. Ho, J. Phys. B **37**, 3177 (2004).
[28] J. Muller, X. Yang, and J. Burgdorfer, Phys. Rev. A **49**, 2470 (1994).
[29] S. Kar, and Y. K. Ho, Phys. Rev. A **72**, 010703(R) (2005).
[30] S. Kar and Y. K. Ho, Chem. Phys. Lett. **402**, 544 (2005).
[31] P. J. Hicks and J. Comer, J. Phys. B **8**, 1866 (1975).
[32] V. A. Mandelshtam, T. R. Ravuri, and H. S. Taylor, Phys. Rev. Lett. **70**, 1932 (1993).
[33] A. Ghoshal and Y. K. Ho, J. Phys. B **42**, 075002 (2009).
[34] J. F. Ritz, J. Reine Angew Math. **135**, 1 (1909).
[35] J. W. Cooper, U. Fano, and F. Prats, Phys. Rev. Lett. **10**, 518 (1963).
[36] S. Kar and Y. K. Ho, J. Phys. B **42**, 044007 (2009).
[37] U. Fano, Nuovo Cimento **12**, 156 (1935).
[38] U. Fano, Phys. Rev. **124**, 1866 (1961).
[39] We would like to thank an anonymous referee for such observation.